Microscopic Study of the Fulde-Ferrell-Larkin-Ovchinnikov State in an All-Organic Superconductor

G. Koutroulakis, H. Kühne, J. A. Schlueter, J. Wosnitza, and S. E. Brown

Microscopic study of the Fulde-Ferrell-Larkin-Ovchinnikov state in an all-organic superconductor

G. Koutroulakis,[1] H. Kühne,[2] J. A. Schlueter,[3] J. Wosnitza,[2,4] and S. E. Brown[1]

[1]*Department of Physics & Astronomy,*

UCLA, Los Angeles, CA 90095, USA

[2]*Hochfeld-Magnetlabor Dresden (HLD-EMFL),*

Helmholtz-Zentrum Dresden-Rossendorf, D-01314 Dresden, Germany

[3]*Materials Science Division, Argonne National Laboratory, Argonne, IL 60439 USA*

[4]*Institut für Festkörperphysik, TU Dresden, D-01069 Dresden, Germany*

Abstract

Quasi-two dimensional superconductors with sufficiently weak interlayer coupling allow magnetic flux to penetrate in the form of Josephson vortices for in-plane applied magnetic fields. A consequence is the dominance of the Zeeman interaction over orbital effects. In the clean limit, the normal state is favored over superconductivity for fields greater than the paramagnetic limiting field, unless an intermediate, inhomogeneous state is stabilized. Presented here are nuclear magnetic resonance (NMR) studies of the inhomogeneous (FFLO) state for β''-$(ET)_2SF_5CH_2CF_2SO_3$. The uniform superconductivity-FFLO transition is identified at an applied field value of 9.3(0.1) T at low temperature ($T = 130$ mK), and evidence for a possible second transition between inhomogeneous states at ~ 11 T is presented. The spin polarization distribution inferred from the NMR absorption spectrum compares favorably to a single-Q modulation of the superconducting order parameter.

PACS numbers: 74.25.Dw,74.25.Kn,74.70.nj

Superconducting charge transfer salts based on the organic donor molecule bisethylenedithio-tetrathiafulvalene (ET) are associated with very anisotropic electronic properties, due to the layered arrangements of ET molecules separated by anionic spacers [1–3]. The details of the planar arrangement provide a classification criterion, allowing for meaningful comparison of physical properties between what are essentially isomorphic compounds. The most familiar polymorph is probably κ-$(ET)_2X$, where the designator κ is associated with a parquet-like arrangement of dimerized ET molecules, and the anions X are polymerized inorganic ligands such as $Cu[N(CN)_2]Br$ and $Cu(NCS)_2$. In comparing the properties amongst those salts, there is clear evidence for the importance of correlations, which are enhanced because of the weak interlayer coupling. This feature, along with the observed long mean free paths [4, 5], make them ideal materials for investigating both the possibility for, and the nature of, field-induced superconducting (SC) phases, stabilized near to and beyond the paramagnetic limiting field B_P [6–12].

In such cases, a first-order phase transition from SC to normal states was predicted, driven by the Zeeman interaction [13]. However, under fairly restrictive circumstances, various intermediate phases were also suggested. The original proposals, by Fulde and Ferrell [14] and independently by Larkin and Ovchinnikov (LO) [15], were made $\sim$50 years ago, and therein the principle mechanism and constraints were identified. Namely, electron pairs acquire a non-zero momentum $\mathbf{q}$ as a consequence of the applied field. For the LO case, the gap oscillates through zero in real-space, $\Delta(\vec{r}) \sim \cos(\vec{Q} \cdot \vec{r})$. In higher than one dimension, the Fermi surface of the compromise state is only partially removed by the pairing. Then, depending on details, such as Fermi surface structure, order parameter symmetry of the low-field SC state (uSC), and field range, single or multiple momentum components are close in energy [16].

Compelling evidence for FFLO physics in real materials is quite recent and restricted to just a few layered molecular superconductors, such as κ-$(ET)_2Cu(NCS)_2$ (hereafter κ-NCS) [8–10, 12] and λ-$(BETS)_2FeCl_4$ [17]. Relevant here is that they are in the clean-limit, remarkably anisotropic, and B_P is accessible (albeit using the resistive magnets of the major facilities). The more familiar magnetic-field coupling to the SC state, which occurs through vortex creation and order parameter suppression in the cores, is avoided for short interlayer coherence and in-plane fields, since flux penetration occurs in the form of Josephson vortices [18, 19], and a straightforward geometric consequence is that the in-plane screening currents

2

fall off as $1/B$ [20].

Most studied is κ-NCS, at the macroscopic level using transport [6, 10], specific heat [7], and torque magnetometry probes [9], and microscopically with ^{13}C NMR spectroscopy [8] and relaxation experiments [12]. The uSC-FFLO boundary was distinct in both types of NMR measurements. The spectroscopy demonstrated the high-field phase was characterized by a sudden increase in both the mean spin polarization $\overline{M}_s(\vec{r})$, and a broad real-space distribution of $M_s(\vec{r})$ while remaining a bulk superconductor. The temperature dependence of the relaxation rate was interpreted as evidence for real-space gap zeroes of an LO state. In considering other systems generally, and the β'' particularly, our aims are several. Since it is just the second candidate system studied microscopically, we consider an NMR investigation central to confirmation of FFLO, since it is specifically sensitive to electron spin states. Moreover, what physics is generic to FFLO or particular to κ-NCS is an open question. Even then, the form of the modulation and how it evolves with field is undetermined. Finally, it is well-known that inhomogeneous phases are sensitive to disorder; with accessible FFLO phases, how the high-field state is impacted should have experimental consequences.

Recent specific heat studies of β''-(ET)$_2$SF$_5$CH$_2$CF$_2$SO$_3$, with $T_c = 4.3$ K, support the FFLO scenario in the range of 9-10 T and above, which is accessible to temporally stable superconducting (rather than resistive) magnets [11]. As a result, where it was not previously possible, the spin polarization on both sides of the transition is inferred from the hyperfine fields. Specifically, reported here are ^{13}C NMR spectroscopy and relaxation (T_1) measurements to 11.9 T. A phase transition is identified at $B_s \simeq 9.3$ T, beyond which significant line-broadening is observed in what is a bulk superconductor. The spectrum is shown consistent with a single-Q modulation. There is considerable local variation in the spatial modulation of the SC gap, which we tentatively associate with the relative importance of disorder in the high-field phase and which could influence the FFLO-normal phase boundary. Finally, the possibility for a 2nd field-induced transition is indicated in the field-dependence of T_1.

ET molecules with ^{13}C spin-labelled on the ET central carbons were used in the electrolytic single-crystal growth of β''-(ET)$_2$SF$_5$CH$_2$CF$_2$SO$_3$. The crystal chosen had well-defined faces, with dimensions approximately 0.8 mm $\times$4.3 mm $\times$0.1 mm and mass 0.9 mg. The long direction is the b-axis, and the shortest dimension is interlayer. Our goal was to collect NMR spectra at low temperature and over as wide a range of calibrated fields

as possible, applied precisely in-plane. For that purpose, the NMR coil was mounted on a piezo-rotator ($\sim 0.001°$ angular steps) with its axis aligned with the long dimension of the crystal. For exploring the SC phase, the sample was cooled to $T < 1$ K in a dilution refrigerator, with the experiment placed directly into the mixing chamber for good thermalization. The NMR experiments were performed using a top-tuning tank circuit, which avoids the problem of inserting mechanically-adjusted circuit elements into the mixing chamber but allows for measurements over a wide field range. A drawback is signal loss due to attenuation in the cable.
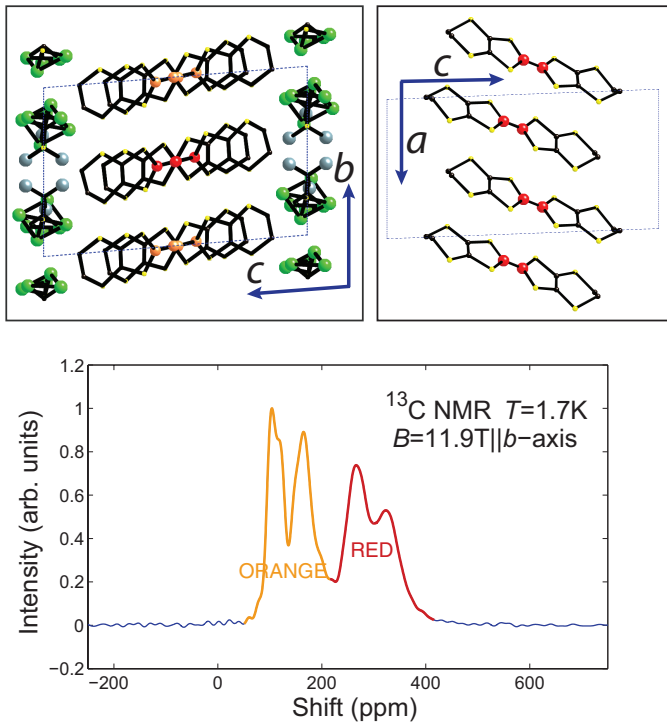

FIG. 1. (*top*) Crystal structure, viewed along [100] (left) and [010] (right) directions. Inequivalent molecules are segregated in stacks aligned with a. The ^{13}C sites are indicated by the colors orange or red, with the *red* molecules sandwiched by the negatively charged SO_3 groups (grey spheres). The associated band structure and Fermi surface are described in the Supplementary Information. (*bottom*) ^{13}C NMR spectrum, recorded at $B = 11.9$ T and $T = 1.7$ K, corresponding to the normal state, with the color-coding indicating the contributions from the *red* and *orange* sites. The applied field is directed precisely in the plane formed by the ET layers, approximately perpendicular to **b**.

^{13}C is commonly introduced into ET donors to probe the hyperfine fields; most effective are the dimer bridging sites. Even then, since carbon is relatively light, the measured para-

4

magnetic shifts are small, typically of order 100-300 ppm relative to the standard reference $(^{13}CH_3)_4Si$ (TMS). In Fig. 1(*top*), the crystal structure is shown, with views along a (left) and b (right). The former emphasizes the layered structure, with ET donors configured in sheets and separated by the organic anions [21]. The labelled ^{13}C ions are highlighted in red and orange for two crystallographically inequivalent molecules. Within the layers, the underlying morphology is aligned stacks of ET donors (into the page). In Fig. 1(*bottom*), a ^{13}C NMR spectrum is shown, recorded at $T = 1.7$ K with magnetic field $B = 11.9$ T, aligned precisely within the layers and approximately perpendicular to b. These conditions correspond to the normal state. In the crystal lattice, the two ^{13}C sites of each of the two molecules are inequivalent, making for four independent sites. The contributions from the two molecules are well-resolved: the absorption from one of the two molecules appears at higher frequency than the other. The distinction arises from a substantial charge carrier imbalance between the two stacks. Our interpretation is that the ET stack sandwiched by the negatively-charged SO_3 ligands of the counterion has the higher hole density, and thus, the greater shift. Following convention [26], we label the two sites within each molecule "inner" and "outer"; the shifts are generally greater for the outer site, because it is positioned closer to the negatively-charged counterion [27]. The contributions are labelled in Fig. 1.

Specific heat measurements have demonstrated the importance of in-plane fields to within less than 1° alignment [11]. Thus, we relied on the angle dependence of normal-core vortex creation and dynamics, which are identifiable through measurements of the RF complex impedance (and in the high-field NMR spectrum [21]). The circuit was tuned and matched (to f=13.4 MHz), and changes to one channel of the complex RF reflection were monitored upon varying the angle of the applied field at T=1.7 K. In Fig. 2(a) is shown results for sweeps in both directions, which includes some hysteresis. The anomaly centered at $\theta = 0$ marks the in-plane condition [28], with the field penetrating as Josephson vortices. Note that the action of the applied RF is to oscillate the field in the plane formed by the dc-field direction and the coil's symmetry axis. Therefore, when aligned, the flux penetration remains in-plane, the Josephson-vortex lattice is weakly pinned, and there is good RF penetration and signal strength despite the superconductivity.

In Fig. 2(c),(d), the field dependence of the absorption spectrum is shown, recorded at T=130 mK, 1.7 K, respectively, and plotted as shift (ppm). At T=130 mK, the onset of the inhomogeneous electron spin polarization occurs for fields exceeding 9.3(0.1) T, marked

by an increase in overall linewidth. At higher fields, the features corresponding to the four inequivalent sites are identifiable. For clarity, the normal-state spectrum of Fig. 1 is also shown as the black dashed trace in Fig. 2(c).

For comparison, the phase diagram determined by specific heat measurements (solid black circles) [11] appears in Fig. 2(b), where the transition between uniform SC (uSC) and FFLO states identified by the NMR results reported here is denoted (blue diamonds/red borders). The vertical red bars indicate the range of fields covered by the NMR measurements, recorded at T=130 mK, 1.7 K.

A first step in quantifying the FFLO state can be found in the ^{13}C first moment NMR shift, $\delta\nu(B)/\nu_0 \equiv (\overline{\nu} - \nu_0)/\nu_0$, with ν_0 the reference frequency (for TMS). At low field and deep in the uSC state, only the orbital part contributes intrinsically to the shift. Whereas, the constant shift of the normal state includes the hyperfine fields associated to the spin susceptibility. Fig. 3(a) depicts the field dependence of $\delta\nu(B)/\nu_0$. The variation between the two limits is associated with the increase of the hyperfine fields, most rapidly at the onset of the inhomogeneous (FFLO) SC phase (blue squares) at $B_s \simeq 9.3$ T. Complementary results for the spin-lattice relaxation rate are shown in Fig. 3(b). Since the ^{13}C magnetization recovery varies considerably over the whole linewidth, what is plotted is the time scale associated with 63% of the full recovery (1-1/e) [29]. Recovery details, and a comparison to what is seen in the κ-NCS material appear in the Supplementary Information.

Ideally, how the high-field SC phase (FFLO) should be interpreted depends in part on our understanding of the low-field phase (uSC) [16, 30], as well as on further evidence for phase transitions within the inhomogeneous phase. The increasing shift for 5-9 T, shown in Fig. 3, is expected in the case of momentum-space nodes. Consider the simple model of a d-wave order parameter with amplitude constrained by the weak-coupling result $2\Delta_0/k_B T_c$=4.3, on a circular Fermi surface. From the resulting Zeeman shift of quasiparticle energies, the result, in the applicable limit $\mu_B B/k_B T \gg 1$, is $M_s/M_n = \mu_B B/2\Delta_0$, with M_s (M_n) the magnetization of the SC (normal) state [31]. Then, $2\Delta_0/k_B \sim 18$ K and $M_s/M_n \approx 4$ %/T, which corresponds to the red line in Fig. 3(a) [32]. (In this context, we note that controversy remains regarding SC states in ET-based superconductors. See, $e.g.$, Refs. [7, 26]).

In relation to the inhomogeneous phase, the observed rapid increase of the shift for $B > B_s = 9.3(0.1)$ T compares favorably to expectations for the onset of an FFLO state in a d-wave superconductor [33], and is similar to prior results from κ-NCS. In addition, here
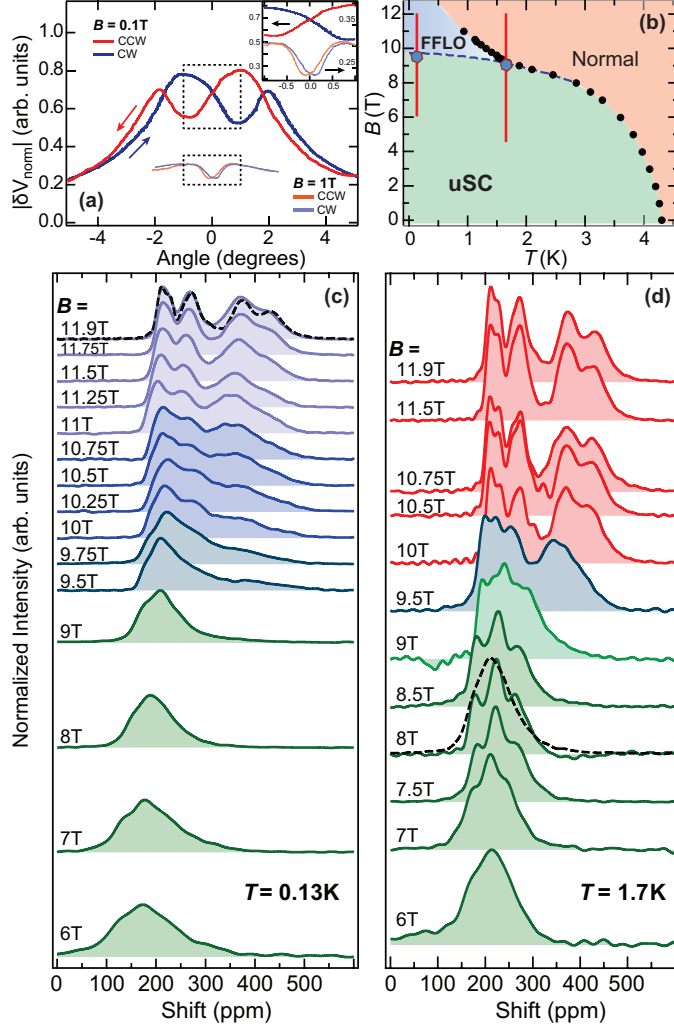
6

FIG. 2. (a) Angle dependence of the reflection signal, with the anomaly at $\theta=0$ associated with the in-plane condition. Hysteresis is reduced upon increasing the field strength. (b) Field/temperature superconductor/normal state phase boundary, as inferred from specific heat measurements (black circles) [11], and the NMR results reported here (blue diamonds). The vertical red bars correspond to the range of field strength for our measurements. (c) Spectral evolution with field, recorded at $T=130$ mK and (d) $T=1.7$ K. At the lower temperature, significant line-broadening is exhibited for fields greater than 9.5T, which we take to be onset of the FFLO phase. For $T=1.7$ K, only the spectrum at 9.5 T takes on a different, transitional, form from what appears at lower and higher fields.
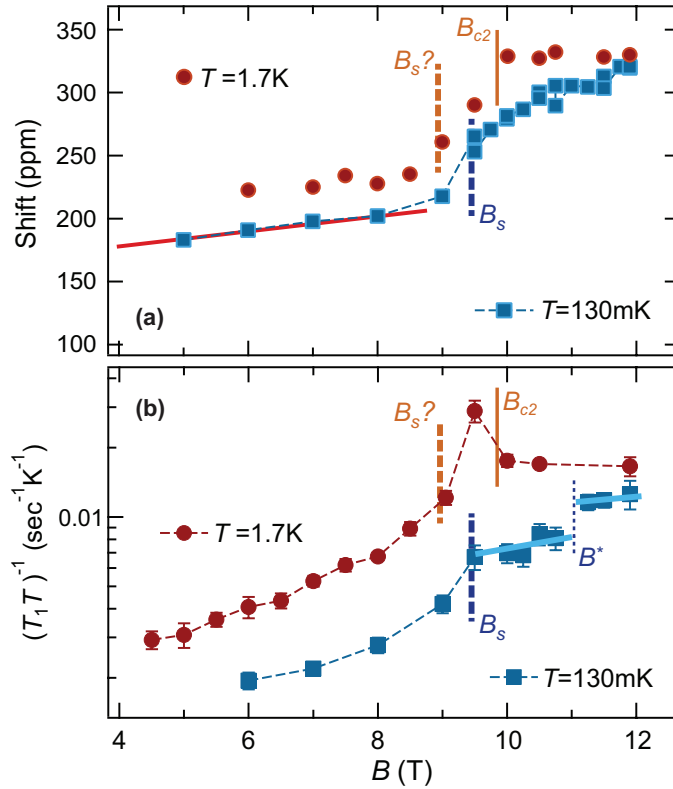
FIG. 3. (a) ^{13}C NMR shift *vs.* B. The solid red line corresponds to the Zeeman effect on a *d*-wave model for circular Fermi surface and weak coupling (see text). Its extrapolation to $B = 0$ leads to a 150 ppm estimate for the orbital shift. (b) Spin-lattice relaxation rate, $T_1^{-1}(B)$. The data recorded at $T = 1.7$ K exhibit an increase at 9.3 T greater than the normal state value, consistent with an incursion into the FFLO phase [12, 21]. The curves connecting the data points are guides-to-the-eye.

there is more than one indication for an additional phase transition at $B^* \sim 11$ T, but with bulk superconductivity surviving to a greater applied field. From Fig. 3(b), the locations of the transitions, *i.e.*, the FFLO onset at $B_s = 9.3$ T and the possibility for another at B^*, have signatures in the field-dependence of T_1^{-1}. Also, for $B > B^*$, the spectral features are seen to narrow considerably (Fig. 2(c)). The evidence for bulk superconductivity persisting at least to 11.9 T at 130 mK appears in Fig. 4, which shows the progressive increase of shift upon warming. Note that the changes are larger for the sites with greater hyperfine fields.

The structure of the FFLO phase may evolve with field, even for simple layered *s*-wave superconductors. For example, in Ref. [16], the sequence of high-field phases for a two-dimensional *s*-wave superconductor is described, where the single-Q phase is destabilized in
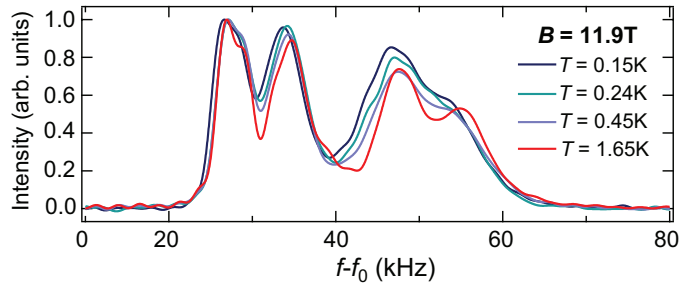
FIG. 4. Temperature dependence of the ^{13}C spectrum, carried out at an applied field $B = 11.9$ T. The variation is due to an increasing hyperfine field upon warming.

favor of double-Q structures. In the case of order parameter nodes, as for a d-wave supercon-ductor and circular Fermi surface, different constraints are imposed on the wavevector and, again, more than one transition is expected within the FFLO state [30]. If this situation were to apply to the β'' superconductor discussed here, it is tempting to assign the lower transition, at B_s, as uSC to FFLO (FFLO$_1$) and the possible upper transition, at B^*, as be-tween inhomogeneous phases FFLO$_1$ and FFLO$_2$. Another possibility is a commensurability effect, associated with locking of the Josephson vortex lattice to the FFLO order parameter phase [17]. Further study is required to confirm the FFLO$_1 \rightarrow$ FFLO$_2$ transition.

The modeling of the inhomogeneous electron spin polarization in the FFLO phase is not unambiguous, since the lineshapes result from four separate contributions with equal total intensity but different hyperfine couplings and local fields. Therefore, we take what is the simplest approach possible, and compare the lineshape to that expected for a single-Q sinusoidal modulation. We are motivated also by the considerable Fermi surface nesting, which tends to favor it [16]. Single-Q modulation is consistent, provided that the idealized lineshape is broadened, for example, by coupling to disorder. The modulation amplitude is fixed to scale with the longitudinal hyperfine coupling of each of the four contributions [21]. We justify this approximate approach as follows. At the FFLO critical field, the order parameter would vary near the zero crossing as an isolated solitonic domain wall of width of the order of the coherence length. However, a soliton lattice forms immediately once moving into the modulated phase, with lattice constant roughly given by the same length scale. At higher fields, the modulation is sinusoidal with progressively weakened amplitude. Then, the modulated part of the spin polarization varies as the modulus of the gap amplitude $|\Delta(x)|^2$. The four contributions are modeled and displayed in Fig. 5 along with their sum,
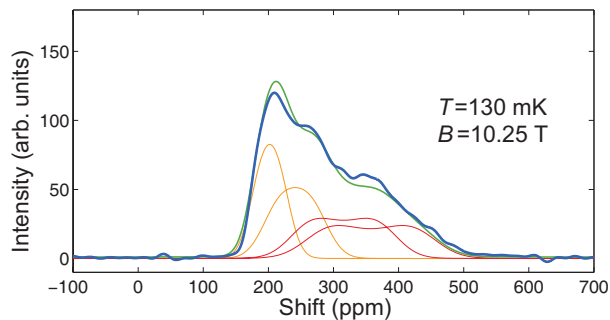
9

FIG. 5. Example of spectrum simulation in the FFLO state, compared to recorded spectrum (blue). The simulation is a sum (green) of four gaussian-broadened contributions (red, orange) arising from a single-Q sinusoidal modulation of the SC order parameter [21].

for contrast to the spectrum recorded at 10.25 T.

In summary, presented here is evidence for a field-induced transition to an inhomogeneous SC phase, an FFLO state, at $B_s = 9.3(0.1)$ T and within the limits of the superconducting phase diagram of the all-organic material β''-$(ET)_2SF_5CH_2CF_2SO_3$. Moreover, a possible second phase transition is identified, between inhomogeneous phases at ~ 11 T. Further study of the field range in the vicinity of 11 T is needed to confirm the latter. The NMR spectra recorded in the modulated phase are consistent with a real-space, single-Q modulation of the order parameter, albeit with substantial broadening.

[1] T. Ishiguro, K. Yamaji, and G. Saito, *Organic Superconductors*, Springer Series in Solid-State Sciences, Vol. 88 (Springer-Verlag, Berlin, 1998).

[2] J. Singleton and C. Mielke, Contemporary Phys. **43**, 63 (2002).

[3] A. G. Lebed, ed., *Organic superconductors and conductors*, Spring Series in Materials Science, Vol. 110 (Springer-Verlag, Berlin, 2008).

[4] J. Wosnitza, *Fermi Surfaces of Low-Dimensional Organic Metals and Superconductors*,

Springer Tracts in Modern Physics, Vol. 134 (Springer Verlag, Berlin Heidelberg, 1996).

[5] J. Singleton, Reports on Progress in Physics **63**, 1111 (2000).

[6] J. Singleton, J. A. Symington, M.-S. Nam, A. Ardavan, M. Kurmoo, and P. Day, J. Phys.: Condensed Matter **12**, L641 (2000).

[7] R. Lortz, Y. Wang, A. Demuer, M. Böttger, B. Bergk, G. Zwicknagl, Y. Nakazawa, and J. Wosnitza, Phys. Rev. Lett. **99**, 187002 (2007).

[8] J. A. Wright, E. Green, P. Kuhns, A. Reyes, J. Brooks, J. Schlueter, R. Kato, H. Yamamoto, M. Kobayashi, and S. E. Brown, Phys. Rev. Lett. **107**, 087002 (2011).

[9] B. Bergk, A. Demuer, I. Sheikin, Y. Wang, J. Wosnitza, Y. Nakazawa, and R. Lortz, Phys. Rev. B **83**, 064506 (2011).

[10] C. C. Agosta, J. Jin, W. A. Coniglio, B. E. Smith, K. Cho, I. Stroe, C. Martin, S. W. Tozer, T. P. Murphy, E. C. Palm, J. A. Schlueter, and M. Kurmoo, Phys. Rev. B **85**, 214514 (2012).

[11] R. Beyer, B. Bergk, S. Yasin, J. A. Schlueter, and J. Wosnitza, Phys. Rev. Lett. **109**, 027003 (2012).

[12] H. Mayaffre, S. Krämer, M. Horvatić, C. Berthier, K. Miyagawa, K. Kanoda, and V. F. Mitrović, Nature Phys. **10**, 928 (2014).

[13] A. M. Clogston, Phys. Rev. Lett. **9**, 266 (1962).

[14] P. Fulde and R. A. Ferrell, Phys. Rev. **135**, A550 (1964).

[15] A. I. Larkin and Y. N. Ovchinnikov, Sov. Phys. JETP **20**, 762 (1965).

[16] Y. Matsuda and H. Shimahara, J. Phys. Soc. Japan **76**, 051005 (2007).

[17] S. Uji, T. Terashima, M. Nishimura, Y. Takahide, T. Konoike, K. Enomoto, H. Cui, H. Kobayashi, A. Kobayashi, H. Tanaka, M. Tokumoto, E. S. Choi, T. Tokumoto, D. Graf, and J. S. Brooks, Phys. Rev. Lett. **97**, 157001 (2006).

[18] P. A. Mansky, P. M. Chaikin, and R. C. Haddon, Phys. Rev. B **50**, 15929 (1994).

[19] J. R. Kirtley, K. A. Moler, J. A. Schlueter, and J. M. Williams, J. Phys.: Condensed Matter **11**, 2007 (1999).

[20] L. Bulaevskii and J. R. Clem, Phys. Rev. B **44**, 10234 (1991).

[21] See Supplemental Material, which includes Refs. [22-25].

[22] R. Beyer and J. Wosnitza, Low Temp. Phys. **39**, 225 (2013).

[23] Q. Cui and K. Yang, Phys. Rev. B **78**, 054501 (2008).

[24] U. Geiser, J. A. Schlueter, H. H. Wang, A. M. Kini, J. M. Williams, P. P. Sche, H. I. Zakowicz,

M. L. VanZile, J. D. Dudek, P. G. Nixon, R. W. Winter, G. L. Gard, J. Ren, and M.-H. Whangbo, J. Am. Chem. Soc. **118**, 9996 (1996).

[25] J. Wosnitza, S. Wanka, J. Hagel, E. Balthes, N. Harrison, J. A. Schlueter, A. M. Kini, U. Geiser, J. Mohtasham, R. W. Winter, and G. L. Gard, Phys. Rev. B **61**, 7383 (2000).

[26] S. M. De Soto, C. P. Slichter, A. M. Kini, H. H. Wang, U. Geiser, and J. M. Williams, Phys. Rev. B **52**, 10364 (1995).

[27] Additional unresolved structure is a splitting of each of the 4 absorption lines arising from ^{13}C-^{13}C dipolar coupling. Its presence is masked here by the relatively greater inhomogeneous line broadening.

[28] J. Shinagawa, Y. Kurosaki, F. Zhang, C. Parker, S. E. Brown, D. Jérome, J. B. Christensen, and K. Bechgaard, Phys. Rev. Lett. **98**, 147002 (2007).

[29] For the distributions of recoveries observed, the distinction from the mean relaxation time $\overline{T_1^{-1}(\nu)}$ is small.

[30] A. B. Vorontsov, J. A. Sauls, and M. J. Graf, Phys. Rev. B **72**, 184501 (2005).

[31] K. Yang and S. L. Sondhi, Phys. Rev. B **57**, 8566 (1998).

[32] Other indications for a nodal order parameter include $T_1^{-1} \sim T^3$ at low fields, and absence of Hebel-Slichter coherence peak for $T < T_c$, to be presented elsewhere.

[33] A. B. Vorontsov and M. J. Graf, AIP Conf. Proc. **850**, 729 (2006).